Putative *BRAF* activating fusion in a medullary thyroid cancer

Katayoon Kasaian,[1] Sam M. Wiseman,[2] Blair A. Walker,[3] Jacqueline E. Schein,[1] Martin Hirst,[1] Richard A. Moore,[1] Andrew J. Mungall,[1] Marco A. Marra,[1,4] and Steven J.M. Jones[1,4,5]

[1]Canada's Michael Smith Genome Sciences Centre, British Columbia Cancer Agency, Vancouver, British Columbia V5Z 4S6, Canada; [2]Department of Surgery, St. Paul's Hospital and University of British Columbia, Vancouver, British Columbia V6Z 1Y6, Canada; [3]Department of Pathology and Laboratory Medicine, St. Paul's Hospital and University of British Columbia, Vancouver, British Columbia V6Z 1Y6, Canada; [4]Department of Medical Genetics, University of British Columbia, Vancouver, British Columbia V6T 1Z4, Canada; [5]Department of Molecular Biology and Biochemistry, Simon Fraser University, Burnaby, British Columbia V5A 1S6, Canada

Abstract Medullary thyroid cancer (MTC) is a malignancy of the calcitonin-producing parafollicular cells of the thyroid gland. Surgery is the only curative treatment for this cancer. External beam radiation therapy is reserved for adjuvant treatment of MTC with aggressive features. Targeted therapeutics vandetanib and cabozantinib are approved for the treatment of aggressive and metastatic tumors that are not amenable to surgery. The use of these multikinase inhibitors are supported by the observed overactivation of the RET oncoprotein in a large subpopulation of MTCs. However, not all patients carry oncogenic alterations of this kinase. Hence, there is still a need for comprehensive molecular characterization of MTC utilizing whole-genome and transcriptome-sequencing methodologies with the aim of identifying targetable mutations. Here, we describe the genomic profiles of two medullary thyroid cancers and report the presence of a putative oncogenic *BRAF* fusion in one. Such alterations, previously observed in other malignancies and known targets of available drugs, can benefit patients who currently have no treatment options.

Corresponding author: sjones@bcgsc.ca

INTRODUCTION

Medullary thyroid cancer (MTC) accounts for 5%–8% of all thyroid cancers, but unlike the majority of thyroid malignancies that are derived from the follicular cells of the gland, MTC represents the malignant transformation of the calcitonin-producing parafollicular C cells (Cerrato et al. 2009). Although 25% of MTCs are hereditary and categorized, depending on the presence of other endocrinopathies, as either familial MTC or multiple endocrine neoplasia type 2 (MEN2) syndrome, the majority of diagnosed cases are sporadic (Flicker et al. 2012). Germline activating point mutations of *rearranged during transfection* (*RET*) are the known causative alterations in >95% of hereditary MTCs; somatic mutations of this oncogene are also found in 50% of sporadic MTCs (Cerrato et al. 2009). Activating somatic mutations of *RAS* genes are found in subpopulations of *RET* mutation-negative sporadic MTCs (Moura et al. 2011; Boichard et al. 2012). Although the majority of studies of MTC have not identified the BRAF V600E activating mutation, commonly implicated in papillary thyroid

cancer (Moura et al. 2011; Boichard et al. 2012; Agrawal et al. 2013), a Korean study and a Greek study have reported the presence of this well-characterized driver alteration in MTC patients (Goutas et al. 2008; Cho et al. 2014). This may be the result of technical variations such as the chosen validation techniques or differences in tissue handling and processing or may be indicative of population-specific cancer drivers.

Five- and 10-yr survival rates in patients diagnosed with MTC are reported at 86% and 78%, respectively, and these plummet to 25% and 10% after discovery of distant metastasis (Schlumberger et al. 2008; Flicker et al. 2012), rendering MTC as more aggressive than the commonly diagnosed follicular-derived thyroid malignancies. MTC is resistant to chemotherapy and radiation therapy and hence complete surgical removal of the thyroid gland is the primary and the most promising curative treatment for localized disease (Flicker et al. 2012). The majority of mortality that occurs due to MTC is, however, due to local and distant metastasis when the primary clinical management of the disease is palliation (Schlumberger et al. 2008). The effectiveness of external beam radiation therapy (EBRT) in the treatment of MTC has been controversial; a study evaluating 66 MTC patients identified in the Surveillance, Epidemiology, and End Results database (SEER; seer.cancer.gov) that were treated with EBRT found that after controlling for known prognostic factors, the overall survival benefit attributed to EBRT in node-positive patients by univariate analysis was lost (Martinez et al. 2010). Radiation therapy is believed to be effective in preventing local disease recurrence only in patients with high-risk features such as the presence of residual disease, nodal positivity, and extranodal cancer extension (Brierley et al. 1996; Fersht et al. 2001; Call et al. 2013). Hence, the American Thyroid Association guidelines for the management of medullary thyroid cancer recommend the use of postoperative EBRT only for those patients at high risk of local disease recurrence to achieve local control (Wells et al. 2015). The Food and Drug Administration has approved the use of the kinase inhibitors vandetanib and cabozantinib for the treatment of advanced medullary thyroid cancer. Vandetanib operates by blocking RET, VEGFRs (vascular endothelial growth factor receptors), and EGFR (epidermal growth factor receptor) (Wells et al. 2012), whereas cabozantinib inhibits the activity of MET (mesenchymal epithelial transition), VEGFR, and RET (Elisei et al. 2013). Although these therapeutics resulted in statistically significant progression-free survival, they do not lead to measurable responses in all patients presenting with advanced and metastatic disease. Additionally, most individuals on treatment who initially respond will eventually progress and die from MTC; thus, there is still a great need for more effective treatments. Here, we provide the genomic analysis of two MTC tumors and report, for the first time, the presence of a putative activating *BRAF* fusion in one of the tumors.

RESULTS

Clinical Presentation and Family History

Patient A is a male of East Indian descent who in 2010 at the age of 33 presented with a left lateral neck mass that by biopsy was diagnosed as an MTC. His serum calcitonin level was 1562 ng/L and his CEA (carcinoembryonic antigen) was 440 µg/L at presentation; he was otherwise asymptomatic. He had no personal or family history of thyroid cancer or other endocrine tumors. He also had no personal history of head and neck radiation exposure. Biochemical screening for parathyroid and adrenal tumors was negative. He underwent a total thyroidectomy, central neck dissection, and selective left lateral neck dissection. At the time of surgery, he was found to have a locally advanced cancer with extensive invasion of his larynx, trachea, esophagus, and the left recurrent laryngeal nerve, which required sacrificing. There were two MTC foci measuring 0.9 and 1.2 cm present in the thyroid and both

were positive for calcitonin and CEA immunohistochemistry. Four of 12 lymph nodes had evidence of metastatic MTC and there was no evidence of extrathyroidal cancer extension. Final staging of his cancer was T4N1bM0. He was treated postoperatively with EBRT. He was followed up by his endocrinologist and radiation oncologist every 4–6 mo and underwent laboratory (calcitonin and CEA) and imaging (CT [computed tomography] of neck, chest, and abdomen) surveillance. During follow-up, he never developed any evidence of structural recurrence. Four years and 11 mo after his operation he was alive and in good health with a calcitonin that was 13 ng/L and a CEA that was 3.1 µg/L, with no gross clinical or imaging evidence of disease.

Patient B, a woman of Scottish/Irish/German descent, was diagnosed at the age of 31 in 2012. She presented with what was believed to be postpartum thyroiditis, and an ultrasound revealed a left 4.7-cm thyroid mass. She had no ultrasound evidence of lateral neck disease. A biopsy of the mass diagnosed MTC. Her serum calcitonin level was 289 ng/L and her CEA was 120 µg/L at presentation. She had no personal history of cancer or head and neck radiation exposure. She had no family history of thyroid cancer or endocrine tumors, although she had a maternal grandmother who had a history of breast cancer that was diagnosed at 48 yr of age. Biochemical screening for parathyroid and adrenal tumors was negative. She underwent a total thyroidectomy and central neck dissection. The MTC measured 2.5 cm, was positive for calcitonin and CEA immunohistochemistry, and had evidence of capsular invasion. There was no evidence of metastases in the eight lymph nodes that were removed from the central neck. Final staging for her cancer was T2N0M0. Postoperatively she was followed up by her endocrinologist every 4–6 mo and underwent laboratory (calcitonin and CEA) and imaging (CT of neck, chest, and abdomen) surveillance. During follow-up, she never developed any evidence of structural recurrence. Three years and 5 mo after her operation, she was alive and in good health with a calcitonin level that was <5 ng/L and a CEA that was <0.5 µg/L, with no gross clinical or imaging evidence of disease.

Genomic Analysis

Whole-genome sequencing of both tumors and matched normal tissues and whole-transcriptome sequencing of both tumors were performed. Genomic profiling of the MTC procured from Patient A at the time of thyroidectomy revealed a very mutationally quiet genome with only seven single-nucleotide somatic variants (Table 1) and no small insertions and deletions, copy-number changes, or large-scale structural alterations. The only evident and known driver mutation in this patient's MTC was the activating p.Q61L KRAS mutation that has previously been described in MTCs (Moura et al. 2011; Boichard et al. 2012; Agrawal et al. 2013). The genome of the MTC procured from Patient B harbored 18 single-nucleotide somatic variants (Table 2). Unlike Patient A's MTC, this genome demonstrated regions of copy-number variation with loss of one copy, and as a result loss of heterozygosity (LOH) of Chromosomes 1p, 4q, 7, 18, 21, and 22 (Fig. 1). We also identified three gene fusions, all resulting from local duplication events (Table 3). A noteworthy fusion was that of *PARP12* and *BRAF* genes. A duplication event on Chromosome 7 led to the fusion of these two genes, producing a putative fusion oncogene with an intact kinase domain; this fusion was expressed and identified in the transcriptome data set. Neither of the MTCs had germline or somatic *RET* mutations. Medullary thyroid cancers show a low mutation rate and in the majority of cases carry only one known driver mutation consistent with an oncogenic addiction profile (Agrawal et al. 2013). Previous studies using low-resolution techniques, such as array comparative genomic hybridization, have also alluded to the rare occurrence of copy-number changes in MTCs and that this cancer can arise without any chromosomal changes or *RET* activating mutations (Flicker et al. 2012) supporting our observations on the whole-genome scale.

**Table 1.** Small somatic variants identified in the tumor genome of Patient A

Gene	Chromosome	HGVS DNA reference	HGVS protein reference	Variant type	Predicted effect	dbSNP ID	Genotype	Read depth	Allele frequency
BIRC6	2	c.10592C>A	p.S3531Y	Substitution	Missense	—	Heterozygous	41	0.1
RUNDC3B	7	c.654G>C	p.E218D	Substitution	Missense	—	Heterozygous	39	0.18
SCGB1C1	11	c.13C>T	p.R5C	Substitution	Missense	rs7951297	Heterozygous	40	0.175
NELL1	11	c.1942A>C	p.S648R	Substitution	Missense	—	Heterozygous	29	0.14
KRAS	12	c.182A>T	p.Q61L	Substitution	Missense	rs121913240	Heterozygous	36	0.22
COPS2	15	c.605T>C	p.D202G	Substitution	Missense	—	Heterozygous	35	0.14
MT-ATP6	MT	c.577T>C	p.F193L	Substitution	Missense	—	Heterozygous	9787	0.04

HGVS, Human Genome Variation Society; dbSNP, Database for Short Genetic Variations.

Table 2. Small somatic variants identified in the tumor genome of Patient B

Gene	Chromosome	HGVS DNA reference	HGVS protein reference	Variant type	Predicted effect	dbSNP ID	Genotype	Read depth	Allele frequency
DUSP10	1	c.392G>A	p.S131N	Substitution	Missense	—	Heterozygous	25	0.48
STAG1	3	c.863T>G	p.M288R	Substitution	Missense	—	Heterozygous	33	0.58
KIF9	3	c.1036A>C	p.T346P	Substitution	Missense	—	Heterozygous	25	0.48
MAP3K4	6	c.3720A>G	p.I1240M	Substitution	Missense	—	Heterozygous	33	0.42
NAMPT	7	c.1456C>G	p.L486V	Substitution	Missense	—	Homozygous	11	1
RGS3	9	c.527T>C	p.V176A	Substitution	Missense	—	Heterozygous	16	0.69
MAMDC4	9	c.1844G>A	p.R615Q	Substitution	Missense	—	Heterozygous	22	0.45
UBE3B	12	c.560C>G	p.P187R	Substitution	Missense	—	Heterozygous	27	0.48
NACA	12	c.3568T>C	p.S1190P	Substitution	Missense	rs2958150	Heterozygous	14	0.29
PSPC1	13	c.1474A>G	p.M492V	Substitution	Missense	rs75085951	Heterozygous	36	0.16
MDP1	14	c.377G>A	p.R126Q	Substitution	Missense	—	Heterozygous	22	0.5
CDRT1	17	c.68T>A	p.I23N	Substitution	Missense	rs201445711	Heterozygous	28	0.18
LOXHD1	18	c.5417T>A	p.H1806L	Substitution	Missense	—	Heterozygous	11	0.18
PLK5	19	—	—	Substitution	Splice site donor	rs10853954	Heterozygous	27	0.44
PSG5	19	c.955G>A	p.E319K	Substitution	Missense	rs17406362	Heterozygous	37	0.51
PES1	22	c.737C>G	p.T246S	Substitution	Missense	—	Heterozygous	9	0.22
MT-ND1	MT	c.106G>A	p.G36S	Substitution	Missense	—	Heterozygous	2722	0.13
MTM1	X	c.700G>A	p.H234Y	Substitution	Missense	—	Heterozygous	33	0.45

HGVS, Human Genome Variation Society; dbSNP, Database for Short Genetic Variations.
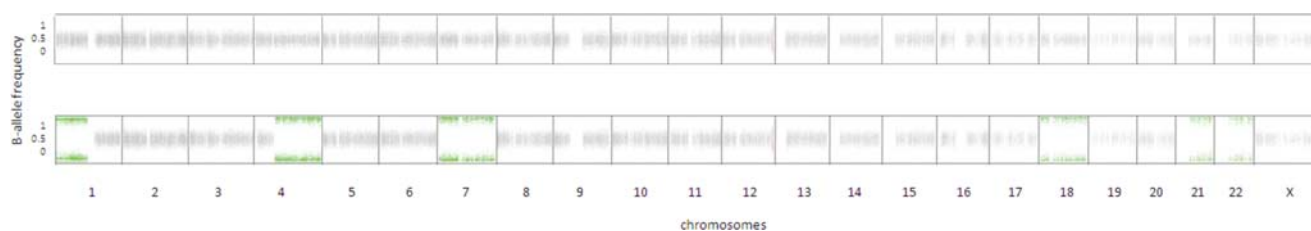
Figure 1. B-allele frequencies (frequency of the alternate allele) of common single-nucleotide polymorphisms (SNPs) in the tumors of Patient A (*top*) and Patient B (*bottom*) are plotted for each chromosome. Although no regions of loss of heterozygosity (LOH) were observed in Patient A, the second patient demonstrated regions of LOH in Chromosomes 1p, 4q, 7, 18, 21, and 22.

DISCUSSION

Surgery is the only curative form of treatment for patients presenting with MTC (Schlumberger et al. 2008). However, persistent disease is observed in 70% of sporadic cases, which are generally resistant to chemotherapy and radiation (Schlumberger et al. 2008). Targeted therapies may thus be the only promising option for the treatment of advanced and refractory MTCs. Half of sporadic MTCs harbor *RET* activating point mutations (Agrawal et al. 2013), and the multikinase inhibitors vandetanib and cabozantinib, which act by blocking the kinase activity of several proteins including RET, are approved for use in the treatment of MTC. These therapies, however, do not lead to measurable responses in all patients with advanced and metastatic disease; detailed analysis of MTC tumors on the genome scale may thus provide clues into yet undefined driver mutations.

In this report, we have described, to the best of our knowledge, the first whole-genome analysis of medullary thyroid carcinoma and the first MTC to harbor a putative oncogenic *BRAF* fusion. Both studied MTCs were considered sporadic disease that lacked somatic (or germline) *RET* alterations. Whole-genome sequence coverage of 30×–40× was produced in the current study (Table 4). Although genome resequencing experiments can rely on an average depth of 35× (Sims et al. 2014), sample and tumor heterogeneity in addition to aneuploid genomes that are observed in almost all cancer specimens require a higher depth of sequence coverage for identifying all relevant somatic mutations. Although the current data sets provided reliable fusion and copy-number profiles at the base-level resolution, they may not have been as robust in describing single-nucleotide variants (SNVs) and small insertions and deletions. Low coverage in the tumor or the matched normal tissue may have resulted in false-negative or false-positive somatic calls, respectively, whereas the studied data sets did not have the power to detect subclonal events.

One patient had an activating *KRAS* mutation; the other lacked any *RAS* mutations but harbored a *BRAF* fusion (Fig. 2). None of the approved targeted therapeutics for MTC shows activity against BRAF, and therefore profiling MTC patients for fusions or other alterations of *BRAF* may warrant the utilization of drugs such as sorafenib, vemurafenib, regorafinib, or

Table 3. Detected gene fusions in the tumor of Patient B

Gene	Genomic breakpoint coordinate	Gene	Genomic breakpoint coordinate	Translated	Event type
BRAF	Chr7:140482184	*PARP12*	Chr7:139728271	Yes	Duplication
TMEM132D	Chr12:129579191	*RIMBP2*	Chr12:130930789	Yes	Duplication
DNAJC17	Chr15:41083978	*RYR3*	Chr15:34113093	No	Duplication

Table 4. Coverage statistics for the sequence libraries

|	Tumor genome coverage	Normal genome coverage	Number of tumor transcriptome reads
Patient A	38×	39× (normal tissue)	149M
Patient B	29×	28× (blood)	284M

M, million.

dabrafenib for the treatment of MTC, contingent on functional validation of these putative oncogenic events. Several BRAF fusions have demonstrated insensitivity to ATP-competitive RAF inhibitors, whereas other in vitro studies showed sensitivity to MEK (mitogen-activated protein kinase kinase) inhibitor therapy; detailed biochemical and clinical characterization of the *BRAF* mutational spectrum is essential for tailored therapeutic intervention (Hutchinson et al. 2013; Sievert et al. 2013; Holderfield et al. 2014). A recent case report described an activating *RET* fusion in a sporadic MTC patient with no *RET* or *RAS* point mutations (Grubbs et al. 2015), and another the presence of *ALK* fusions in two MTC patients (Ji et al. 2015). These studies and our report of the *BRAF* fusion suggest a need for more comprehensive profiling of these tumors and the utilization of techniques capable of detecting large-scale structural events such as gene fusions.

Currently upon presentation and depending on the institutional practices, MTC patients may be tested for the presence of point mutations in *RET*, activation of which leads to the activation of downstream signaling pathways including RAS–RAF–ERK and PI3K–AKT pathways. Mutations of various members of the same signaling pathway can exert a similar effect on the phenotype, and thus *RET* mutation-negative MTCs may harbor alterations of other signaling proteins in these networks. Such pathway-level mutual exclusivity has been observed in papillary thyroid cancers where *RET* fusions, *BRAF*, and *RAS* activating mutations were not found together in any tumor; all, however, are members of the same signaling pathway (Cancer Genome Atlas Research Network 2014). Cancer cases with no *RET* point mutations may harbor alterations such as oncogenic gene fusions of other members of its signaling pathways. More effective targeted treatment can thus be made possible through comprehensive mutational profiling of key signaling molecules in cancer pathways.

METHODS

DNA from the two flash-frozen MTC tumors and matched normal specimens were subjected to whole-genome sequencing; 100-bp paired-end sequence reads were generated on
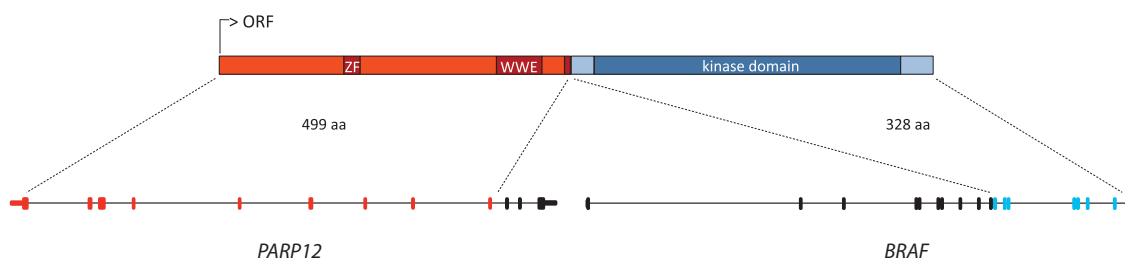
Figure 2. Duplication on Chromosome 7 resulted in an in-frame fusion of *PARP12* and *BRAF* genes in the MTC tumor of Patient B producing a putative fusion oncogene harboring *PARP12* exons 1–9 and *BRAF* exons 11–18. ORF, open reading frame; ZF, zinc finger; WWE, Trp-Trp-Glu.

Illumina HiSeq2500 instruments following the manufacturer's protocol with minor variations. In addition, 75-bp paired-end transcriptome sequence reads were produced for the tumors (Table 4).

Sequence reads from the whole-genome libraries were aligned to the human reference genome (build GRCh37) using the Burrows–Wheeler alignment (BWA) tool (Li and Durbin 2010). The tumor's genomic sequence was compared with that of the patient's constitutive DNA to identify somatic alterations. Regions of copy-number variation and LOH were determined using hidden Markov model–based approaches HMMcopy and APOLLOH (Ha et al. 2012), respectively. De novo assembly and annotation of genomic data using ABySS and Trans-ABySS (Simpson et al. 2009) were used to identify small insertions and deletions (indels) and large structural variants (SVs) including translocations, inversion, and duplications leading to gene fusions; identified SVs were verified using an orthogonal alignment–based detection tool, BreakDancer (Chen et al. 2009). Single-nucleotide variants and indels in the tumor/normal pair were identified using a probabilistic joint variant calling approach utilizing SAMtools and Strelka (Li et al. 2009; Saunders et al. 2012). Sequence reads from the transcriptome libraries were aligned to the human reference genome (build GRCh37) using TopHat (Kim et al. 2013) with Ensembl gene model annotation file on the -G parameter. The reference sequence and the corresponding annotation files were provided by Illumina's iGenome project and downloaded from the TopHat homepage (http://ccb.jhu.edu/software/tophat/index.shtml). Structural variants were identified using a de novo assembly-based approach using ABySS and Trans-ABySS (Simpson et al. 2009) and the alignment-based SV detection tool MOJO (Minimum Overlap Junction Optimizer; https://github.com/cband/MOJO).

ADDITIONAL INFORMATION

Ethics Statement

The patient specimens were collected as part of a research project approved by the British Columbia Cancer Agency's Research Ethics Board. Both patients provided written informed consent for the complete genomic profiling of their specimens.

Database Deposition and Access

The aligned sequence data sets have been deposited at the European Genome-phenome Archive (EGA; http://www.ebi.ac.uk/ega/) under accession number EGAS00001001473. The *BRAF* fusion sequence is deposited at GenBank (http://www.ncbi.nlm.nih.gov/genbank) under accession number KU221508. The *KRAS* mutation is deposited at the ClinVar database (http://www.ncbi.nlm.nih.gov/clinvar) under accession number SCV000257452.

Acknowledgments

Author Contributions

S.M.W., M.A.M., and S.J.M.J. conceived and designed the study. K.K. performed data analysis and wrote the manuscript. B.A.W. provided pathology review. J.E.S., M.H., R.A.M., and A.J.M. accrued specimens and performed library constructions and sequencing.

REFERENCES

Agrawal N, Jiao Y, Sausen M, Leary R, Bettegowda C, Roberts NJ, Bhan S, Ho AS, Khan Z, Bishop J, et al. 2013. Exomic sequencing of medullary thyroid cancer reveals dominant and mutually exclusive oncogenic mutations in RET and RAS. *J Clin Endocrinol Metab* **98:** E364–E369.

Boichard A, Croux L, Al Ghuzlan A, Broutin S, Dupuy C, Leboulleux S, Schlumberger M, Bidart JM, Lacroix L. 2012. Somatic RAS mutations occur in a large proportion of sporadic RET-negative medullary thyroid carcinomas and extend to a previously unidentified exon. *J Clin Endocrinol Metab* **97:** E2031–E2035.

Brierley J, Tsang R, Simpson WJ, Gospodarowicz M, Sutcliffe S, Panzarella T. 1996. Medullary thyroid cancer: analyses of survival and prognostic factors and the role of radiation therapy in local control. *Thyroid* **6:** 305–310.

Call JA, Caudill JS, McIver B, Foote RL. 2013. A role for radiotherapy in the management of advanced medullary thyroid carcinoma: the Mayo Clinic experience. *Rare Tumors* **5:** e37.

Cancer Genome Atlas Research Network. 2014. Integrated genomic characterization of papillary thyroid carcinoma. *Cell* **159:** 676–690.

Cerrato A, De Falco V, Santoro M. 2009. Molecular genetics of medullary thyroid carcinoma: the quest for novel therapeutic targets. *J Mol Endocrinol* **43:** 143–155.

Chen K, Wallis JW, McLellan MD, Larson DE, Kalicki JM, Pohl CS, McGrath SD, Wendl MC, Zhang Q, Locke DP, et al. 2009. BreakDancer: an algorithm for high-resolution mapping of genomic structural variation. *Nat Methods* **6:** 677–681.

Cho U, Oh WJ, Bae JS, Lee S, Lee YS, Park GS, Lee YS, Jung CK. 2014. Clinicopathological features of rare BRAF mutations in Korean thyroid cancer patients. *J Korean Med Sci* **29:** 1054–1060.

Elisei R, Schlumberger MJ, Müller SP, Schöffski P, Brose MS, Shah MH, Licitra L, Jarzab B, Medvedev V, Kreissl MC, et al. 2013. Cabozantinib in progressive medullary thyroid cancer. *J Clin Oncol* **31:** 3639–3646.

Fersht N, Vini L, A'Hern R, Harmer C. 2001. The role of radiotherapy in the management of elevated calcitonin after surgery for medullary thyroid cancer. *Thyroid* **11:** 1161–1168.

Flicker K, Ulz P, Höger H, Zeitlhofer P, Haas OA, Behmel A, Buchinger W, Scheuba C, Niederle B, Pfragner R, et al. 2012. High-resolution analysis of alterations in medullary thyroid carcinoma genomes. *Int J Cancer* **131:** E66–E73.

Goutas N, Vlachodimitropoulos D, Bouka M, Lazaris AC, Nasioulas G, Gazouli M. 2008. BRAF and K-RAS mutation in a Greek papillary and medullary thyroid carcinoma cohort. *Anticancer Res* **28:** 305–308.

Grubbs EG, Ng PK, Bui J, Busaidy NL, Chen K, Lee JE, Lu X, Lu H, Meric-Bernstam F, Mills GB, et al. 2015. RET fusion as a novel driver of medullary thyroid carcinoma. *J Clin Endocrinol Metab* **100:** 788–793.

Ha G, Roth A, Lai D, Bashashati A, Ding J, Goya R, Giuliany R, Rosner J, Oloumi A, Shumansky K, et al. 2012. Integrative analysis of genome-wide loss of heterozygosity and monoallelic expression at nucleotide resolution reveals disrupted pathways in triple-negative breast cancer. *Genome Res* **22:** 1995–2007.

Holderfield M, Deuker MM, McCormick F, McMahon M. 2014. Targeting RAF kinases for cancer therapy: BRAF-mutated melanoma and beyond. *Nat Rev Cancer* **14:** 455–467.

Hutchinson KE, Lipson D, Stephens PJ, Otto G, Lehmann BD, Lyle PL, Vnencak-Jones CL, Ross JS, Pietenpol JA, Sosman JA, et al. 2013. BRAF fusions define a distinct molecular subset of melanomas with potential sensitivity to MEK inhibition. *Clin Cancer Res* **19:** 6696–6702.

Ji JH, Oh YL, Hong M, Yun JW, Lee HW, Kim D, Ji Y, Kim DH, Park WY, Shin HT, et al. 2015. Identification of driving ALK fusion genes and genomic landscape of medullary thyroid cancer. *PLoS Genet* **11:** e1005467.

Kim D, Pertea G, Trapnell C, Pimentel H, Kelley R, Salzberg SL. 2013. TopHat2: accurate alignment of transcriptomes in the presence of insertions, deletions and gene fusions. *Genome Biol* **14:** R36.

Li H, Durbin R. 2010. Fast and accurate long-read alignment with Burrows–Wheeler transform. *Bioinformatics* **26:** 589–595.

Li H, Handsaker B, Wysoker A, Fennell T, Ruan J, Homer N, Marth G, Abecasis G, Durbin R; 1000 Genome Project Data Processing Subgroup. 2009. The sequence alignment/map format and SAMtools. *Bioinformatics* **25:** 2078–2079.

Martinez SR, Beal SH, Chen A, Chen SL, Schneider PD. 2010. Adjuvant external beam radiation for medullary thyroid carcinoma. *J Surg Oncol* **102:** 175–178.

Moura MM, Cavaco BM, Pinto AE, Leite V. 2011. High prevalence of RAS mutations in RET-negative sporadic medullary thyroid carcinomas. *J Clin Endocrinol Metab* **96:** E863–E868.

Saunders CT, Wong WS, Swamy S, Becq J, Murray LJ, Cheetham RK. 2012. Strelka: accurate somatic small-variant calling from sequenced tumor-normal sample pairs. *Bioinformatics* **28:** 1811–1817.

Schlumberger M, Carlomagno F, Baudin E, Bidart JM, Santoro M. 2008. New therapeutic approaches to treat medullary thyroid carcinoma. *Nat Clin Pract Endocrinol Metab* **4:** 22–32.

Sievert AJ, Lang SS, Boucher KL, Madsen PJ, Slaunwhite E, Choudhari N, Kellet M, Storm PB, Resnick AC. 2013. Paradoxical activation and RAF inhibitor resistance of BRAF protein kinase fusions characterizing pediatric astrocytomas. *Proc Natl Acad Sci* **110:** 5957–5962.

Simpson JT, Wong K, Jackman SD, Schein JE, Jones SJ, Birol I. 2009. ABySS: a parallel assembler for short read sequence data. *Genome Res* **19:** 1117–1123.

Sims D, Sudbery I, Ilott NE, Heger A, Ponting CP. 2014. Sequencing depth and coverage: key considerations in genomic analyses. *Nat Rev Genet* **15:** 121–132.

Wells SA Jr, Robinson BG, Gagel RF, Dralle H, Fagin JA, Santoro M, Baudin E, Elisei R, Jarzab B, Vasselli JR, et al. 2012. Vandetanib in patients with locally advanced or metastatic medullary thyroid cancer: a randomized, double-blind phase III trial. *J Clin Oncol* **30:** 134–141.

Wells SA Jr, Asa SL, Dralle H, Elisei R, Evans DB, Gagel RF, Lee N, Machens A, Moley JF, Pacini F, et al. 2015. Revised American Thyroid Association guidelines for the management of medullary thyroid carcinoma. *Thyroid* **25:** 567–610.